THE JOURNAL OF PHYSICAL CHEMISTRY B

Article

pubs.acs.org/JPCB

Supramolecular Interactions between Inorganic and Organic Blocks of Pentacyanoferrate/Poly(4-vinylpyridine) Hybrid Metallopolymer

Sergio Augusto Venturinelli Jannuzzi, Bianca Martins, Maria Isabel Felisberti, and André Luiz Barboza Formiga*

Institute of Chemistry, P.O. Box 6154, University of Campinas − UNICAMP, 13083-970, Campinas, SP, Brazil

ABSTRACT: The combination of organic and inorganic molecular building blocks gives rise to hybrid supramolecular materials showing properties from both chemical domains. This work presents the synthesis of metallopolymers made from poly(4-vinylpyridine) (P4VP) and pentacyanoferrate(II) at various polymer repeating unit/$[Fe(CN)_5]^{3-}$ ratios (py/Fe) and focuses on the influence of each block on the properties of the other. The solvatochromic shift of the $[Fe(CN)_5]^{3-}$ moiety was investigated as a function of the py/Fe ratio and the water molar fraction (X_{H_2O}) of the ethanol/water medium. Asymmetric solvation favoring ethanol was enhanced as the py/Fe ratio increased. The results lead to a modification of the well-established thermodynamical model for asymmetrical solvation and suggest the formation of water-rich domains within the polymer coils with a large number of $[Fe(CN)_5]^{3-}$ units. From the macromolecular perspective, the increase of $[Fe(CN)_5]^{3-}$ units resulted in higher values of intrinsic viscosity, which is rationalized by the increase of the polymer coil charge density and therefore the increase in hydrodynamic volume due to repulsive electrical forces. Evaluating the intrinsic viscosity of a sample with py/Fe = 25 in solvent mixtures with different water molar fractions, it was found that the hydrodynamic volume is maximized at intermediate X_{H_2O} values, where both the ethanol-soluble uncomplexed polymer block and the water-soluble $[Fe(CN)_5]^{3-}$-pendant units can be suitably solvated, preventing coil shrinkage.

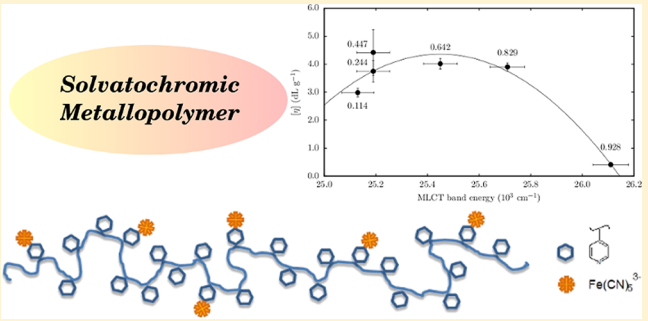

INTRODUCTION

The combination of organic and inorganic domains in a hybrid material is a promising approach toward new functionalities, which may arise either from the synergistic interaction between the different domains or from the simple addition of the properties of both domains in a single matrix. The incorporation of metal ions and coordination compounds in organic polymers allows the specific properties of the metallic centers, such as catalytic, electronic, magnetic, electrochromic, and luminescence capabilities, to be imparted onto a macromolecular scale.[1,2] The latter properties, usually related to molecules dissolved in a solution, are now able to be incorporated onto lyophobic polymeric colloidal particles, surfaces of micelles,[3] or multilayered architectures,[4] for example, where they may yield new molecular-designed functional materials.

In general, metallopolymers can be synthesized in three different ways: by living polymerization of a metal-containing monomer,[5] by reaction between metal ions and a preformed polymer bearing coordinating heteroatoms,[6] or by supramolecular polymerization between a doubly functional organic spacer and a metal ion.[7] The first approach demands a careful study of the reaction conditions to control chain growth. On the other hand, the last two approaches seem to be more readily applicable to coordination compounds, since the organic moiety might be thought of as a macromolecular ligand. Thus, the knowledge from traditional coordination chemistry is now applicable to facilitate metallopolymer synthesis. The metal−macroligand interaction is an unexplored field because the macromolecular nature of the ligand may lead to modification of the chemical environment, may interfere in the stability and kinetics, and may be used for supramolecular self-assembly, for instance.

A problem that had to be faced at the early stages of incorporation of metals into polymers was the lack of solubility of the products.[1] However, the pair poly(4-vinylpyridine) (P4VP) and pentacyanoferrate(II) showed the advantage of being soluble over a reasonable range of water/methanol compositions. This fact allowed Anson and collaborators,[8] at the beginning of the 1980s, to produce coated electrodes by casting homogeneous solutions of the metallopolymer with known composition. This procedure turned out to be an advantage with respect to reproducibility over other poly(4-vinylpyridine)-based systems reported in earlier papers of the same group,[9] where the electrochemical responses were determined by the coating procedure. During the 1990s, other papers[10] on the electrochemistry of P4VP−$[Fe(CN)_5]^{3-}$ metallopolymer were published.

Received: August 29, 2012
Revised: December 3, 2012
Published: December 4, 2012

   dx.doi.org/10.1021/jp308583a | J. Phys. Chem. B 2012, 116, 14933−14942

Recognizing that the earlier papers were focused on metallopolymer electrochemistry, the present work aims to describe this system in solution from a supramolecular point of view, to perceive how each block of the same metallomacromolecule interferes with the properties of the other. The solvatochromic shift of the $[Fe(CN)_5]$ moiety was investigated, giving information about the polarity of its chemical environment, as well as the intrinsic viscosity of dilute solutions, which is related to the hydrodynamic volume of the metallopolymer coil.

EXPERIMENTAL SECTION

Materials. All reagents were used as received from commercial sources, with no further purification.

Synthesis of $Na_3[Fe(CN)_5NH_3]\cdot 3H_2O$. The inorganic block precursor sodium aminopentacyanoferrate(II) has a labile ammonia ligand that was designed to be displaced by the pendant pyridyl moieties of P4VP. The procedure was based on sodium nitroprusside (99%, Merck) in concentrated ammonium hydroxide (28%, Sigma Aldrich), as described in the literature.[11] The reaction yield was 87%. The FTIR spectrum shows intense and asymmetric bands at 2035, 2046, and 2089 cm^{-1} related to vibration modes involving C≡N stretching that are expected for complexes of $[Fe^{II}(CN)_5L^n]^{n-3}$.[12] Additionally, bands related to the amino group are observed at 3380−3250, 1653, 1265, and 712 cm^{-1}. They are attributed to ν(NH), $\delta_d(NH_3)$, $\delta_s(NH_3)$ and $\rho_r(NH_3)$, respectively. The amount of crystallyzation water molecules was calculated by thermogravimetric analysis. Elemental analysis resulted in C 17.92% (18.42%), H 2.75% (2.78%), and N 25.36% (25.78%), where expected values are in paretheses.

Synthesis of $Na_3[Fe(CN)_5py]\cdot 3H_2O$. The complex sodium pyridylpentacyanoferrate(II) was prepared in order to serve as a reference compound for the pentacyanoferrate bound to the pyridyl moieties of the P4VP chain. A 0.5 g (1.45 mmol) portion of sodium aminopentacyanoferrate(II) was dissolved in 2.5 mL of distilled water, and 2.5 mL of a 3 mol L^{-1} aqueous solution of pyridine (99%, Queel Indústrias Químicas S. A.) was added. The mixture was cooled in an ice bath for 30 min in the dark. The precipitation of the yellow solid started by adding 5.0 g (33 mmol) of NaI (99.9+%, Merck) and was completed after addition of 80 mL of ethanol. The precipitate was filtered, washed with ethanol, and recrystallized three times. After that, the thick yellow paste was placed in a clean vial and dried in a desiccator containing phosphorus pentoxide. The reaction yield was 50%. The FTIR spectrum exhibits strong, asymmetric bands related to ν(CN) at 2050 and 2042 cm^{-1} with a shoulder at 2021 cm^{-1}. A band at 1625 cm^{-1} is assigned to CN vibrations in the pyridinic ring, while two weak bands in the 2850−2930 cm^{-1} range are evidence of ring CH stretching.

Synthesis of the Metallopolymers. Initially, 5.0 mL of a poly(4-vinylpyridine) (99%, M_w = 160 000, Aldrich) stock solution in ethanol with a concentration of 422 mmol L^{-1} of the polymer repeating unit (44.4 g L^{-1} of P4VP) is placed in a round-bottom flask and is deaerated by flowing nitrogen for 15 min. An aliquot of a 123 mmol L^{-1} aqueous solution of $Na_3[Fe(CN)_5py]\cdot 3H_2O$ is added, and the mixture is stirred at room temperature for 2 h. The aliquot volume was chosen to achieve a desired polymer repeating unit/pentacyanoferrate molar ratio (py/Fe). The samples are labeled as $[Fe(CN)_5(P4VP)_S]$, with S representing the py/Fe ratio. The chosen values, along with solution volumes are shown in Table 1. During the stirring, a small amount of water was added to homogenize the forming metallopolymer solution. After that, the flask's atmosphere was saturated with nitrogen and it was stored at 8 °C in order to slow decomposition. The integrity of the samples of up to 3 weeks was attested by UV−vis spectroscopy.

Table 1. The P4VP−$[Fe(CN)_5]^{3-}$ Metallopolymer Samples Prepared

sample name	py/Fe molar ratio	volume of $[Fe(CN)_5]^{3-}$ solution[a] (mL)	volume of P4VP solution[b] (mL)	volume of water added (mL)
$[Fe(CN)_5(P4VP)_5]$	5	3.441	5.00	1.3
$[Fe(CN)_5(P4VP)_{10}]$	10	1.721	5.00	1.6
$[Fe(CN)_5(P4VP)_{25}]$	25	0.688	5.00	2.2
$[Fe(CN)_5(P4VP)_{50}]$	50	0.344	5.00	2.0
$[Fe(CN)_5(P4VP)_{75}]$	75	0.229	5.00	2.0
$[Fe(CN)_5(P4VP)_{100}]$	100	0.172	5.00	2.0
$[Fe(CN)_5(P4VP)_{200}]$	200	0.086	5.00	2.1
$[Fe(CN)_5(P4VP)_{400}]$	400	0.043	5.00	2.0

[a] 123 mmol L^{-1} in water. [b] 422 mmol L^{-1} in ethanol.

Infrared Spectroscopy. FTIR analyses of the complexes and of the dried ground metallopolymers were performed in a ABB Bomen MB Series spectrophotometer using KBr pellets in the range 400−4000 cm^{-1}. The pure P4VP film could not be suitably ground; thus, the spectrum was acquired in total reflection mode by a Smiths Illuminati IR II infrared microprobe in the range 650−4000 cm^{-1}. The spectrum intensity was corrected by the equipment's software to allow comparison with FTIR spectra.

Solvatochromic Measurements. An aliquot of the freshly prepared metallopolymer solution was transferred to a 3.5 mL quartz cuvette with 1 cm of optical length. Distilled water or ethanol was added in order to achieve a desired water molar fraction for the solvent. The solution was diluted using a water/ethanol mixture of the same water molar fraction until the concentration of pentacyanoferrate(II) reached 2.5×10^{-4} mol L^{-1} so that the absorbance was in the range of unity. After sample preparation, the cuvette was placed in a HP Agilent 8453 ultraviolet−visible spectrophotometer and the spectrum was acquired in the range 200−1100 nm. The procedure was done for at least seven different water molar fractions for each of the samples listed in Table 1.

Capillary Viscosimetry Measurements. The viscosimetry was performed in a Cannon−Fenske capillary viscosimeter immersed in a thermostatized water bath at 25 °C. After 10 min of thermostatization, the flow time was measured with a chronometer at least three times, with less than 1% of deviation between them. The intrinsic viscosity was calculated on the basis of four dilutions of each of the samples listed in Table 1.

RESULTS AND DISCUSSION

Metallopolymer Formation. A key feature of metallopolymer formation is the different solubilities of its constituents in the solvents used. Sodium aminopentacyanoferrate(II) is soluble in water but not in ethanol, whereas P4VP is not soluble in water but is in ethanol. Due to this fact, the mixtures of both solutions immediately phase separate into a milky white bottom phase and a clean yellow upper phase. However, a few minutes later, the mixture becomes homogeneous, indicating that the product of the reaction depicted in Figure 1 is soluble in the water/ethanol medium.

dx.doi.org/10.1021/jp308583a | J. Phys. Chem. B 2012, 116, 14933−14942

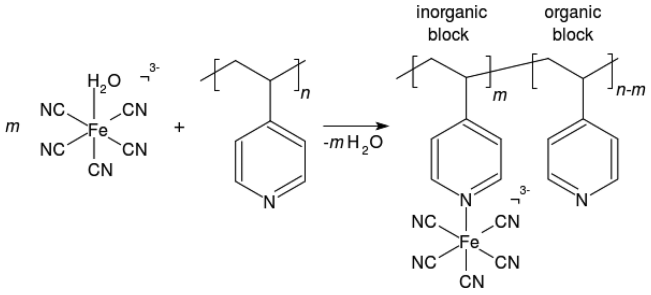

Figure 1. In aqueous solution, the ammonia ligand of sodium pentacyanoferrate(II) is readily displaced by water,[13,14] which comprises the labile ligand to be displaced by the pyridyl moieties of the P4VP chain. The inorganic molecular block is depicted as the metal-containing chain units and the organic block as the metal-free chain segments.

Other evidence of pentacyanoferrate(II)−polymer complexation may be inferred from the infrared spectra shown in Figure 2. A strong band at 2044 cm^{-1} attributed to ν(CN) stretching of cyanide bound to Fe^{II} is observed on metallopolymer spectra.[15] All samples also show a less intense band at 2112 cm^{-1} that might be attributed to stretching of cyanide bound to Fe^{III}.[15] This observation suggests a partial oxidation of the pendant pentacyanoferrate(II) groups. Bands attributed to symmetric and asymmetric $\nu(CC_{ring})$ and $\nu(CN_{ring})$ of the pyridyl groups were shifted after complexation, in accordance with reports[16−18] of P4VP interacting with Lewis acids. The simple protonation is capable of raising the wavenumber of P4VP pyridinic ring stretching from 1595 to 1634 cm^{-1}.[16] In the presence of a didodecylbenzenesulphonate zinc complex, this band is shifted to 1617 cm^{-1},[17] and with Tb^{3+}, it goes to 1606 cm^{-1}, while $\nu_a(CC_{ring})$ shifts from 1415 cm^{-1} in pure P4VP to 1425 cm^{-1} after Tb^{3+} complexation.[18] One can notice in Figure 2b that the band at 1595 cm^{-1} of P4VP is shifted to 1603 cm^{-1} after addition of pentacyanoferrate. Besides, the band at 1413 cm^{-1} is also shifted to 1421 cm^{-1}, in close similarity with the Tb^{3+} complex.[18] The observed band shifts to higher wavenumber corroborate the complexation between pentacyanoferrate and the pendant pyridinic ring of P4VP.

The UV−vis spectrum in the visible region of the aqueous solution of the reference complex $Na_3[Fe(CN)_5py]$ is characterized by a metal-to-ligand charge transfer (MLCT) band with a molar absorptivity of (3.7−4.0) × 10^3 L mol^{-1} cm^{-1},[19] as shown in Figure 3. The spectrum of P4VP has no absorption in the visible range, whereas the metallopolymer samples exhibited an absorption in the same region as the reference complex. The average molar absorptivity was 4.1 × 10^3 L mol^{-1} cm^{-1}. These facts are strong evidence of the presence of pentacyanoferrate(II) bound to pendant pyridyl groups of the polymer. Figure 3 shows the spectrum of $[Fe(CN)_5(P4VP)_{25}]$ as an example.

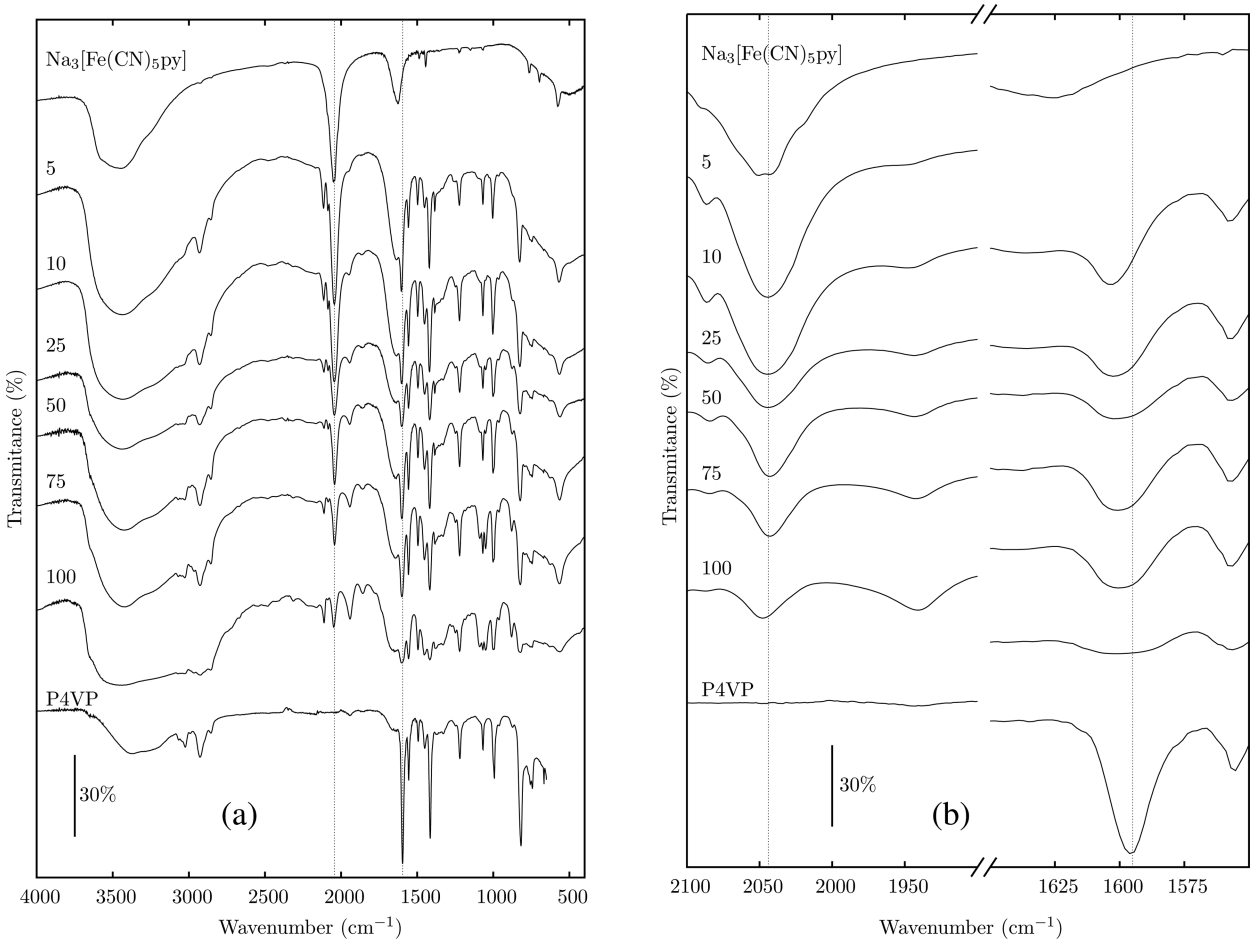

Figure 2. (a) Infrared spectra of the metallopolymers, reference complex, and pure P4VP. (b) Zoom in the region 1550−2100 cm^{-1} showing the ν(CN) stretching band and shift of the band from 1595 to 1603 cm^{-1}.

dx.doi.org/10.1021/jp308583a | J. Phys. Chem. B 2012, 116, 14933−14942

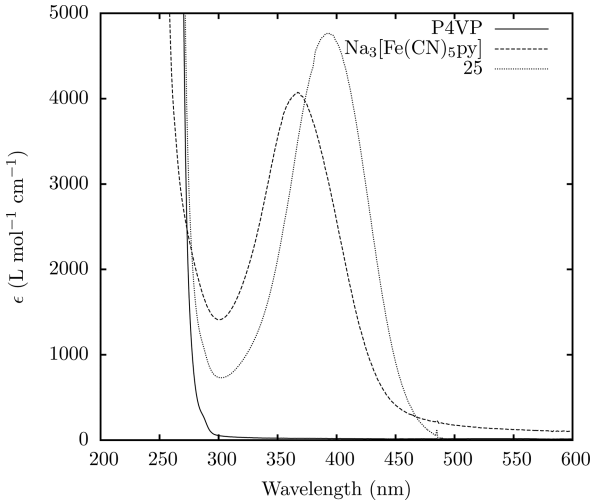

Figure 3. Absorption spectra from the ultraviolet−visible region of poly(4-vinilpyridine) (P4VP), of the reference complex $Na_3[Fe(CN)_5py]$, and of the metallopolymer sample $[Fe(CN)_5(P4VP)_{25}]$.

The actual amount of complexed pentacyanoferrate could be estimated by comparing the absorption band intensity in the visible region with the expected intensity, considering total conversion of aminopentacyanoferrate into pyridinic pendant groups. The actual values ranged from 75 to 90% of the added amount, indicating the reaction yield of metallopolymer formation depicted in Figure 1. These values agree with reaction yields of aminopentacyanoferrate with aromatic *N*-heterocycles.[14,20]

Although the band intensity matched, its position varied between the metallopolymer samples from 26 316 to 25 000 cm^{-1} (380−410 nm) and was red-shifted compared to the band of the reference complex at 27 248 cm^{-1} (367 nm).[19] Such differences were the evidence that each py/Fe ratio yielded a metallopolymer with a different strength of solvatochromism because each sample was synthesized in a solvent with a different water molar fraction.

Solvatochromism. The solvatochromic effect is present in pentacyanoferrate due to the unhomogeneous charge distribution over the molecule; furthermore, the electronic states involved in MLCT are not identically solvated. Recent studies assign MLCT to a $A_1 \leftarrow A_1$ transition, which comprises charge transfer from the d_{xz} orbital of Fe to the $\pi^*_{b_1}$ orbital of the *N*-heterocycle aromatic ligand, in agreement with the literature.[21] Hydrogen bond formation leads to stabilization of the ground state, causing an increase of the $Fe(d\pi) \rightarrow py(\pi^*)$ transition energy, as depicted in Scheme 1. In this way, pentacyanoferrate anion acts as a probe of the chemical environment polarity within the polymer coil.

When the medium is composed of a mixture of two solvents, one might ideally expect pentacyanoferrate solvation to be random; i.e., molecules of both solvents (water or ethanol) are equally likely to compose the solvation shell of the complex. In this case, the composition of the solvation shell is the same as the bulk solvent. Thus, the MLCT wavenumber in the mixed solvent medium (ν^S) may be expressed by a linear combination of the transition wavenumber in pure water (ν_w) and in pure ethanol (ν_e) weighted by each solvent's molar fraction (X_w and X_e). Thus, if the transition wavenumber ν^S is plotted as a function of the solvent's water molar fraction (X_w), a straight line is expected, as expressed in eq 1.

Scheme 1. Effect of the Hydrogen Bonds at the Cyanides in the Energy of the 3dπ Orbitals of the $[Fe(CN)_5]^{3-}$ Moiety and Its Effect on the Metal-to-Ligand Charge Transfer (MLCT) Transition

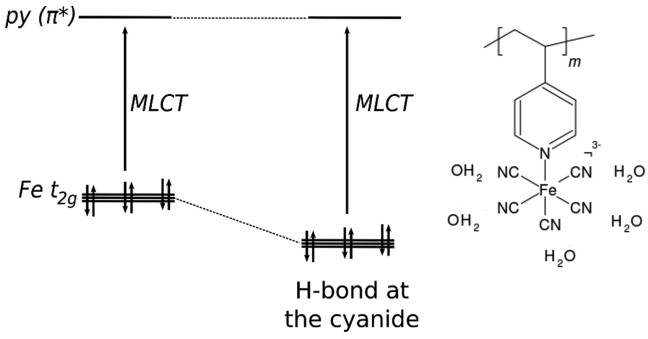

$$\nu^S = X_w\nu_w + X_e\nu_e \quad \therefore \quad \nu^S = X_w(\nu_w - \nu_e) + \nu_e \qquad (1)$$

On the other hand, usually the solute is preferentially solvated by one of the solvent components. In this case of asymmetric solvation, the composition of the solvation shell might differ from the composition of bulk solvent that was controlled experimentally. Then, the plot $\nu^S \times X_w$ will deviate from the ideal straight line pointing to the solvent that is more abundant in solvation shell compared to bulk solution.

Figure 4 presents the plot of $\nu^S \times X_w$ for the reference complex $Na_3[Fe(CN)_5py]$ as well as for each metallopolymer

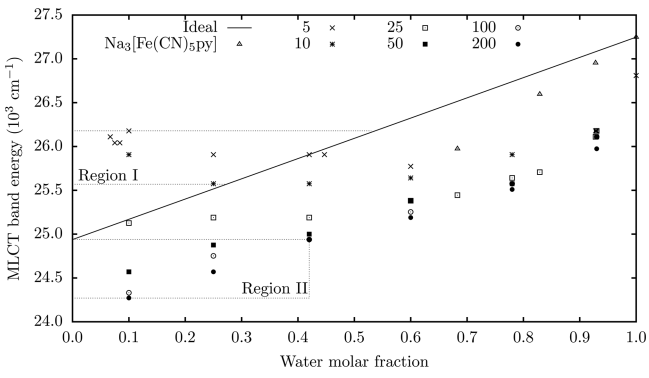

Figure 4. Wavenumbers of the metal-to-ligand charge transfer band as a function of water molar fractions of the water/ethanol solvent for the various samples investigated. The ideal behavior of random solvation is represented by a straight line and the model complex $Na_3[Fe(CN)_5py]$ by a dotted triangle. The numbers are the py/Fe ratios of the metallopolymer samples, with the respective symbols.

sample, differing only by the py/Fe ratio. The ideal straight line was obtained by eq 1 using the values of ν_w and ν_e of the reference complex, which equals 27 248 cm^{-1} (367 nm) and 24 938 cm^{-1} (401 nm), respectively.[21]

The region of X_w above 0.42 is characterized by having the wavenumber of all samples under the ideal straight line. This means that the transition energy in this region is closer to the energy of $[Fe(CN)_5py]^{3-}$ in pure ethanol than in pure water. Consequently, the pentacyanoferrate moieties are preferentially solvated by ethanol rather than water. Toma and Takasugi[21] showed that many cyanoferrates, including $[Fe(CN)_5py]^{3-}$, are preferentially solvated by solvents such as methanol, ethanol, dimethylformamide, or dimethylacetamide in binary mixtures of these solvents and water. The observed deviation and the

dx.doi.org/10.1021/jp308583a | J. Phys. Chem. B 2012, 116, 14933−14942

Table 2. Preferential Solvation Constant for Water/Ethanol Calculated Using the Original and the Modified Model as Well as $x_{w(B)}$ for the Latter

	original model[a]		modified model[b]		
sample name	$K_{w/e}$	R^2	$K'_{w/e}$	$x_{w(B)}$	R^2
ideal	1	1	1	0	1
$Na_3[Fe(CN)_5py]$	0.53 ± 0.02	0.994	0.56 ± 0.02	0[d]	0.999
$[Fe(CN)_5(P4VP)_5]$	0.10 ± 0.02	0.204[c]	0.052 ± 0.004	0.48 ± 0.03	0.982
$[Fe(CN)_5(P4VP)_{10}]$	0.23 ± 0.03	0.028[c]	0.12 ± 0.01	0.27 ± 0.03	0.983
$[Fe(CN)_5(P4VP)_{25}]$	0.095 ± 0.006	0.914	0.093 ± 0.006	0.08 ± 0.01	0.966
$[Fe(CN)_5(P4VP)_{50}]$	0.081 ± 0.006	0.948	0.073 ± 0.007	0.07 ± 0.04	0.974
$[Fe(CN)_5(P4VP)_{75}]$	0.080 ± 0.004	0.974	0.077 ± 0.006	0[d]	0.979
$[Fe(CN)_5(P4VP)_{100}]$	0.080 ± 0.004	0.977	0.077 ± 0.007	0[d]	0.979
$[Fe(CN)_5(P4VP)_{200}]$	0.064 ± 0.004	0.963	0.060 ± 0.006	0[d]	0.969

[a]Equation 2. [b]Equation 3. [c]Low correlation coefficient values indicate low correlation to eq 2. [d]Fitting yielded statistically not representative values, which are thus indicated by zero.

preferential solvation by ethanol of the metallopolymer containing the pyridyl–$[Fe(CN)_5]^{3-}$ bond is thus expected because it reproduces the behavior of the model complex $[Fe(CN)_5py]^{3-}$.

It is interesting to note, however, that, increasing the number of polymer repeating units per pentacyanoferrate unit causes the extent of downward deviation to increase. The model complex, which is py/Fe = 1, lies close to the ideal straight line, the metallopolymer with py/Fe = 10 lies in the mid part, and the data of the py/Fe = 200 sample lies lower than all others. It is worth remembering that the P4VP chain is only soluble in ethanol but not in water and the pentacyanoferrate solubility is the opposite. This observation suggests that the longer the extent of the ethanol-soluble P4VP chain, the more ethanol molecules solvate the metallopolymer chain and consequently the solvation shells of pentacyanoferrate units anchored at the coil are enriched with ethanol. This is evidence that the polarity of the chemical environment of the polymer coil is tuned by the amount of bound pentacyanoferrate.

At X_w lower than 0.42, the plot of Figure 4 exhibits two anomalous regions marked as I and II. Investigations of both regions lead to different ranges of polarity of the polymer coil chemical environment and will be discussed in separated sections.

Deviations at Low py/Fe Ratio. In region I, the data of the samples $[Fe(CN)_5(P4VP)_5]$ and $[Fe(CN)_5(P4VP)_{10}]$ cross the ideal straight line and approach the transition wavenumber of the complex immersed in water. This means that the preferential solvation is no longer with ethanol but water. Toma and Takasugi[21] have pointed out that, at lower water concentrations, water–solute interactions favor solvation by water. Probably, in such low concentrations, it is not possible for water to be stabilized in bulk solution by forming polymeric and polyhedral arrangements sustained by hydrogen bonds, making their interaction with $[Fe(CN)_5]^{3-}$ more energetically favorable, where hydrogen bonds can be formed with nonbonding electron pairs of cyanide or neighboring molecules of the solvation shell.

The upward crossing of data points does not occur at samples with higher py/Fe ratios, indicating that a higher concentration of $[Fe(CN)_5]^{3-}$ units is necessary for water stabilization on their solvation shells. One can consider the formation of water-rich domains within the metallopolymer coil assisted by the closeness of $[Fe(CN)_5]^{3-}$ units in the samples $[Fe(CN)_5(P4VP)_5]$ and $[Fe(CN)_5(P4VP)_{10}]$ at low water molar fractions.[22] Inside these so-called "water pockets", water molecules might arrange themselves in a more stable fashion than in the bulk solution due to interactions with $[Fe(CN)_5]^{3-}$ units and their Na^+ counterions. In addition, the formation of water pockets may somehow be unfavorable when the $[Fe(CN)_5]^{3-}$ concentration is low, probably because of the greater distance between them, making their approximation to form a hydrophilic domain unlikely.

In order to investigate the pictorial hypothesis described above, a modification on the traditional thermodynamic model for asymmetric solvation[23] is proposed. The original model considers the solvation shell to be composed of independent sites which are always occupied by the solvent molecules that can be partitioned between the solvation shell and bulk solvent according to eq 2.

$$K_{w/e} = \frac{x_w/x_e}{X_w/X_e} \quad \therefore \quad \frac{x_w}{x_e} = K_{w/e}\frac{X_w}{X_e} \tag{2}$$

Here, x_w and x_e are the molar fractions of water and ethanol in the solvation shell and X_w and X_e are the molar fractions in bulk solvent. It is possible to estimate x_w/x_e directly from the plots of Figure 4, as described elsewhere,[21] and plots of x_w/x_e as a function of X_w/X_e should yield a straight line with slope $K_{w/e}$. In the case of ideal random solvation, the composition of the solvation shell and bulk solvent is the same; thus, the preferential solvation constant for water/ethanol ($K_{w/e}$) equals unity.

The consideration of solvent sites being independent implies that the occupation of each one has no influence on the occupation of an adjacent site in the same solute molecule or in a nearby molecule. This consideration seems reasonable when the solute molecules are well dispersed throughout the solution, when interactions between them are less likely. As a consequence of the macromolecular nature of the P4VP ligand, many $[Fe(CN)_5]^{3-}$ units are bound to the same polymer chain, prohibiting free dispersion and confining them in a small volume, where interactions between solvation shells of nearby pentacyanoferrate units become more likely to happen.

We now shall consider two different sites composing the solvation shell: one type which is independent, like those in the original model (A sites), and another where solvation depends on the proximity of $[Fe(CN)_5]^{3-}$ units (B sites). Water molecules are capable of forming two hydrogen bonds, so they must be more likely than ethanol molecules to suffer influence of nearby hydrogen-bond forming species. Therefore, the B sites contain water that will establish water-rich domains on the

dx.doi.org/10.1021/jp308583a | J. Phys. Chem. B 2012, 116, 14933–14942

polymer coil through hydrogen bond chains of the type Fe−CN···(HOH···Na^+···)$_u$(HOH···)$_p$NC−Fe. Mathematically, we still intend to use the original thermodynamic formulation described by Frankel and co-workers in the original model,[23] i.e., taking into consideration only independent sites (A sites). Thus, the water fraction in A sites is the total water fraction, subtracting water in B sites: $x_{w(A)} = x_w - x_{w(B)}$. Substituting this modification in eq 2, we have

$$K'_{w/e} = \frac{(x_w - x_{w(B)})/x_e}{X_w/X_e} \quad \therefore \quad \frac{x_w}{x_e} = K'_{w/e}\frac{X_w}{X_e} + \frac{x_{w(B)}}{x_e} \tag{3}$$

When the bulk solvent is water poor ($X_w \to 0$), the water molar fraction in the solvation shell equals $x_{w(B)}$, meaning that this amount of water composes the hydrophilic domains suggested in the pictorial hypothesis. Table 2 presents the results of experimental data of Figure 4 fitted to eqs 2 and 3.

Both $K_{w/e}$ and $K'_{w/e}$ are less than unity, indicating preferential solvation by ethanol and confirming the downward shift depicted in Figure 4 at X_w above 0.42. The preferential solvation constant values of the metallopolymers are smaller than those of the model complex $Na_3[Fe(CN)_5py]$. This is evidence that the macromolecular nature of the ligand imparts to the $[Fe(CN)_5]^{3-}$ moiety a more hydrophobic environment. The covalent bonds of the polymer chain keep segments of free polymer repeating units in the vicinity of units complexed with $[Fe(CN)_5]^{3-}$ groups, thereby bringing to the cyanoferrate more ethanol molecules because the free P4VP chain is only soluble in ethanol.

Comparing the metallopolymer samples, the preferential solvation constant values decrease when the $[Fe(CN)_5]^{3-}$ content decreases (increasing py/Fe ratio). This confirms that the lower the amount of $[Fe(CN)_5]^{3-}$ units, the larger is the ethanol-only soluble organic block and consequently more ethanol is present in the $[Fe(CN)_5]^{3-}$ solvation shell. In other words, the polarity of the chemical environment of $[Fe(CN)_5]^{3-}$ is tuned by the amount of pentacyanoferrate bounded to the P4VP chain.

Samples with py/Fe ratios in the range 200 to 25 exhibited similar values of $K_{w/e}$ and $K'_{w/e}$. The fitting quality expressed by R^2 of these data is approximately constant for the modified model but decreases in the case of the original model when the pentacyanoferrate content increases, especially at py/Fe ratios of 10 and 5. This fact indicates that at low pentacyanoferrate concentrations the assumption of independent sites holds, but it becomes less acceptable at higher concentrations where the considerations made in the modified model are required.

The asymmetric solvation constants $K_{w/e}$ and $K'_{w/e}$ are markedly different for samples of py/Fe ratios 10 and 5, which are the same as those presenting the upward crossing. Besides, the fitting quality indicates that the original model cannot successfully describe the experimental data, which are suitably described by the modified model. The success of fitting data of highly concentrated samples suggests that the assumption of water pocket formation is reasonable and may take place under certain conditions of X_w and py/Fe ratios.

For the samples of py/Fe ratios 25, 10, and 5, the water molar fractions of the hydrophilic domains ($x_{w(B)}$, Table 2), calculated by the modified model, agree quite well with the experimental values of X_w where the upward crossing at Figure 4 is observed. This agreement corroborates the hypothesis of a spontaneous inversion of preferential solvation of $[Fe(CN)_5]^{3-}$ units followed by formation of water-rich domains attached to the metallopolymer coils with the water content $x_{w(B)}$ in the limit of water molar fraction in bulk solution tending to zero.

Deviations at High py/Fe Ratio. Deviations due to high pentacyanoferrate concentrations have been discussed so far. At the opposite concentration range, another unexpected solvatochromic behavior is indicated in region II in Figure 4. At X_w = 0.42, the MLCT energies of the samples with py/Fe ratios of 75, 100, and 200 are the same as for $Na_3[Fe(CN)_5py]$ immersed in pure ethanol, indicating that at these conditions only ethanol molecules compose the pendant complex's solvation shell. At lower bulk solution water molar fraction, the MLCT energy is even lower, which might be interpreted as the complex lying in an even more apolar chemical environment. In other words, the complex is interacting with the polymer chains, as if it was solvating them.

Decreasing X_w, the MLCT energy continues to decrease, indicating that the interaction with the P4VP chain is gradually becoming higher. In this case, one may consider region II as if the complex was being solvated by ethanol and by polymer repeating units. In order to determine the MLCT energy of pentacyanoferrate interacting ideally only with the polymer chain in the absence of ethanol and water, a thin film of the solution of $[Fe(CN)_5(P4VP)_{200}]$ was cast. After drying under nitrogen, the thin film UV−vis spectrum was acquired, revealing the MLCT band at 24 272 cm^{-1} (412 nm). By having the energies in pure ethanol and in pure P4VP, the preferential solvation treatment can be applied to characterize the range of low polarities of the complex chemical environment.

Following the original model, an equation analogous to eq 2 can be written as

$$K_{e/p} = \frac{x_e/x_p}{X_e/X_p} \quad \therefore \quad \frac{x_e}{x_p} = K_{e/p}\frac{X_e}{X_p} \tag{4}$$

where the asymmetric solvation constant of ethanol/polymer medium ($K_{e/p}$) can be estimated.

The values of $K_{e/p}$ presented in Table 3 show that the polymer is the preferential solvent and that the higher the py/Fe ratio, the greater is the preference for solvation by polymer repeating units. This observation was expected, since the complex is soluble in pyridine (which is similar to P4VP repeating units) but not in ethanol. Besides, ethanol molecules interact well with the P4VP chain, so the longer the extent of the pristine P4VP chain, the better is the interaction with ethanol molecules, which no longer solvate $[Fe(CN)_5]^{3-}$ moieties.

Table 3. Preferential Solvation Constants of Region II of Figure 4, Considering the $[Fe(CN)_5]^{3-}$ Units of the Metallopolymer Dissolved in a Mixture of Ethanol and P4VP Chain

sample name[a]	$K_{e/p}$	R^2
$[Fe(CN)_5(P4VP)_{50}]$	0.15 ± 0.01	0.990
$[Fe(CN)_5(P4VP)_{75}]$	0.07 ± 0.01	0.942
$[Fe(CN)_5(P4VP)_{100}]$	0.036 ± 0.005	0.937
ideal	1	1

[a]Calculation for sample $[Fe(CN)_5(P4VP)_{200}]$ was not possible due to lack of experimental data points.

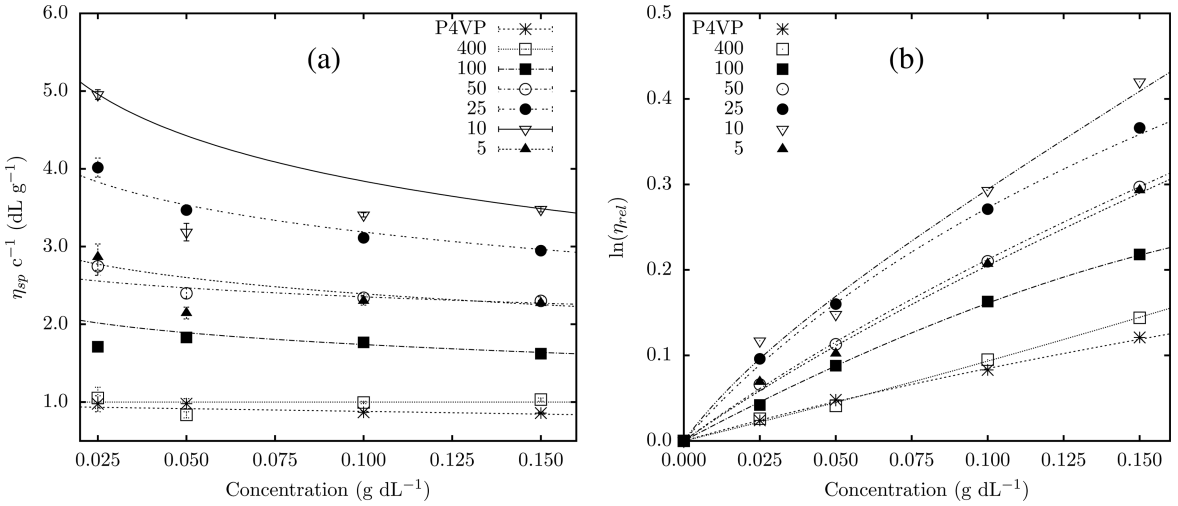

Figure 5. Evaluation of experimental data according (a) to eq 9 and (b) to eq 10. Experimental data of samples $[Fe(CN)_5(P4VP)_{200}]$ and $[Fe(CN)_5(P4VP)_{75}]$ were omitted for clarity.

Macromolecular Coil Conformation in Solution. Since the influence of the polymer on the spectroscopic properties of the complex has been studied, our attention turns now to the opposite point of view: the influence of the complex on the rheological properties of the macromolecule. A simple and reliable way to probe the macromolecular coil extension or contraction is through capillary viscosimetry. When a dilute solution flows inside a capillary tube, the macromolecular coil is subjected to a shear force field due to the solvent velocity gradient arising from the tube wall pointing to its center. As a result, the coil rotates and increases the friction with solvent molecules, leading to increased solution viscosity. If the coil is expanded due to good solvent−polymer interactions or due to electrostatic repulsion of polymer segments, the increment is larger than if the coil is compacted like a rigid sphere.[24]

The increment of polymer solution viscosity (η), compared to solvent viscosity (η_0), is expressed in terms of the specific viscosity (η_{sp}), which is related to the flow time of the polymer solution (t) and of the pure solvent (t_0) by eq 5. This equation holds true neglecting the change in solution density due to polymer addition, by using Poiseuille's equation.[25]

$$\eta_{sp} = \frac{\eta - \eta_0}{\eta_0} = \eta_{rel} - 1 = \frac{t - t_0}{t_0} \tag{5}$$

Dividing by the polymer concentration c, the coil intrinsic viscosity ($[\eta]$) is defined as

$$[\eta] = \lim_{\substack{c\to 0\\ \dot{\gamma}\to 0}} \frac{\eta_{sp}}{c} \tag{6}$$

i.e., in the limit of infinite dilution and in the absence of shear rate. $[\eta]$ states for the hydrodynamic volume of 1 g of macromolecules in solution if they were composed only by isolated coils in equilibrium.[26] In terms of macromolecular dimensions, intrinsic viscosity is expressed as[27]

$$[\eta] = \frac{5}{2}\frac{N_A}{M}\lim_{\substack{c\to 0\\ \dot{\gamma}\to 0}} V_h \tag{7}$$

where N_A and M are Avogadro's number and molar mass, respectively, and V_h is the coil hydrodynamic volume.

The values of $[\eta]$ can be determined by graphic extrapolation of curves of η_{sp}/c as functions of c. For neutral polymers, this curve is usually a straight line and Huggins' equation[28] is generally employed (eq 8).

$$\frac{\eta_{sp}}{c} = [\eta] + k_H[\eta]^2 c \tag{8}$$

However, if the polymer coil bears fixed electric charges, which is the case of P4VP−$Fe(CN)_5$ metallopolymers, the curve η_{sp}/c vs c shows a sharp increase when c tends to zero by virtue of the electroviscous effect.[29−31] Because of this, Fuoss[32] has proposed an equation that is widely accepted for polyelectrolytes (eq 9).

$$\frac{\eta_{sp}}{c} = \frac{[\eta]}{1 + B\sqrt{c}} \tag{9}$$

where B is a measure of polyion−counterion interaction.[32a] Further papers[31,33,34] report that, at even lower polymer concentrations, η_{sp}/c values reach a maximum and fall off, in disagreement with eq 9. The reason for the occurrence of this maximum has been investigated,[35−37] but it was recognized that there is still no physical meaning for such a maximum,[36] even though many electrostatic-based mathematical models[35,38,39] have tried to adequately describe the viscosity of polyelectrolyte solutions.

Since an exact description from first principles is complicated, simplifying assumptions are made, such as graphical extrapolation, which presents an inherent inconsistency. While the polymer concentration goes to zero, the difference $\eta - \eta_0$ also approaches zero, leading to a zero divided by zero indetermination of models represented by eq 8,[28] eq 9,[32] and others.[25,35]

In order to shed light on the problem of a reliable evaluation of $[\eta]$, a recent approach[26] based on phenomenological thermodynamics developed an equation (eq 10) that does not suffer from indetermination and which is applicable to solutions of both uncharged and charged polymers and to linear or branched macromolecules.[40]

$$\ln \eta_{rel} = \frac{c[\eta] + Bc^2[\eta][\eta]^\bullet}{1 + Bc[\eta]} \tag{10}$$

where B here represents the hydrodynamic interaction between segments belonging to different macromolecules,[41] in analogy

dx.doi.org/10.1021/jp308583a | J. Phys. Chem. B 2012, 116, 14933−14942

Table 4. Intrinsic Viscosities and Fitting Parameters of P4VP−$Fe(CN)_5$ Metallopolymers[a]

	eq 9		eq 10		
sample name	$[\eta]$ (dL/g)	B (dL/g)$^{1/2}$	$[\eta]$ (dL/g)	B	$[\eta]^\bullet$ (dL/g)
P4VP	0.95 ± 0.05[b]	−0.7 ± 0.4	1.02 ± 0.06	3.8 ± 0.9	0.4 ± 0.6
$[Fe(CN)_5(P4VP)_{400}]$	1.0 ± 0.1[b]	0[e]	0.86 ± 0.08	0[e]	1.5 ± 0.5
$[Fe(CN)_5(P4VP)_{200}]$	0.94 ± 0.07[b]	2.8 ± 0.5	0.90 ± 0.08	0[e]	3.8 ± 0.9
$[Fe(CN)_5(P4VP)_{100}]$	2.4 ± 0.3[c]	1.2 ± 0.5	1.88 ± 0.04	0[e]	4.0 ± 0.2
$[Fe(CN)_5(P4VP)_{75}]$	2.3 ± 0.1[c]	0.4 ± 0.2	2.06 ± 0.03	0[e]	4.4 ± 0.2
$[Fe(CN)_5(P4VP)_{50}]$	2.8 ± 0.3[d]	0.6 ± 0.4	2.6 ± 0.1	1.8 ± 0.3	1.1 ± 0.8
$[Fe(CN)_5(P4VP)_{25}]$	4.8 ± 0.3[d]	1.6 ± 0.3	4.0 ± 0.2	1.5 ± 0.1	0.6 ± 0.9
$[Fe(CN)_5(P4VP)_{10}]$	7.0 ± 0.8[d]	2.6 ± 0.7	4.8 ± 0.2	4.6 ± 2.8	2.1 ± 0.2
$[Fe(CN)_5(P4VP)_5]$	3.3 ± 0.5[d]	1.2 ± 0.7	2.5 ± 0.3	2.4 ± 1.3	1.3 ± 0.2

[a]Correlation coefficients of fitting with eq 9 ranged from 0.84 to 0.99, while with eq 10 they lied all above 0.99. [b]Obtained by linear extrapolation. All data points probably lied before the maximum. Values of B are angular coefficients of the linear extrapolation. To P4VP, it is equivalent to k_H of eq 8. [c]Obtained by eq 9 excluding the point at 0.25 g/L because it lied before the maximum. [d]Obtained by eq 9 with all data points. [e]Fitting yielded statistically not representative values, which are thus indicated by zero.

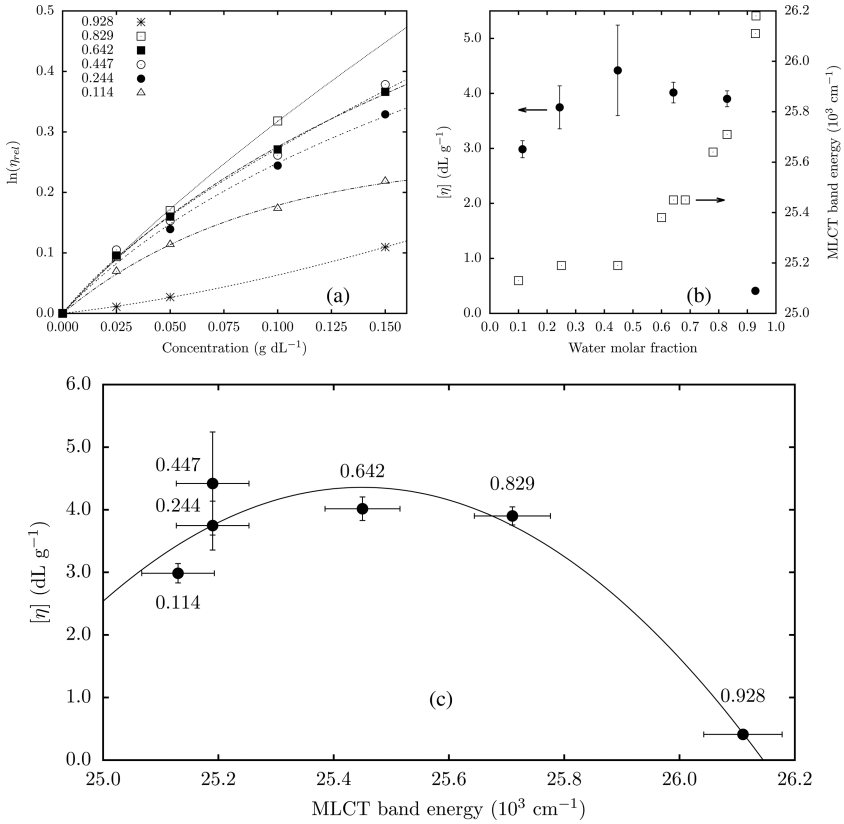

Figure 6. (a) Natural logarithm of relative viscosity as a function of concentration of $[Fe(CN)_5(P4VP)_{25}]$ solution, (b) intrinsic viscosity and MLCT band energy as a function of solvent water molar fraction, and (c) intrinsic viscosity as a function of MLCT band energy. The solvent's water molar fractions are indicated over the points.

to k_H of eq 8, and $[\eta]^\bullet$ is a characteristic specific hydrodynamic volume or simply an adjustable parameter required for polyelectrolytes.[26,41] Both the well-known eq 9 and the novel eq 10 were applied to our data for the sake of comparison, as shown in Figure 5. Intrinsic viscosities evaluated by both equations and other fitting parameters are shown in Table 4.

Note that the application of eq 9 had some complications, as expected from the existence of a maximum in the plots of samples with high py/Fe ratios. On the other hand, eq 10 was applied to all data points with better correlation, denoting a more general equation. Comparing $[\eta]$ values given by both equations, one can note that those obtained by eq 9 are frequently higher. This fact was also reported by Wolf and co-workers[26] and may be due to problems in the limit of infinite dilution.

Metallopolymers with py/Fe ratios of 400 and 200 presented intrinsic viscosities close to pure P4VP due to the low degree of modification. Increasing the pentacyanoferrate content, the intrinsic viscosity also increases, showing that the macromolecule responds to the coordination of $[Fe(CN)_5]^{3-}$ moieties by expanding the coils. Such an expansion might be attributed to electrostatic repulsion between unscreened charged pentacyanoferrate groups along with steric hindrance between them, taking into account the volume of their counterions and solvation shells.

dx.doi.org/10.1021/jp308583a | J. Phys. Chem. B 2012, 116, 14933−14942

Interestingly, intrinsic viscosity values reach a maximum at a py/Fe ratio of 10. Further coordination of $[Fe(CN)_5]^{3-}$ groups causes the polymer coil to shrink. The reason for this might be the increase of ionic strength due to the presence of more ionic pendant groups and Na^+ counterions within the coil and to an increase of uncoordinated pentacyanoferrate. The origins of uncoordinated pentacyanoferrate—probably in the form of an aquocomplex—are dissociation from the metallopolymer due to its lability[14] and incomplete reaction with the polymer, as described earlier.

Another hypothesis to explain the decrease of intrinsic viscosity values at high pentacyanoferrate content is the fact that highly charged linear polyelectrolytes tend to assume an extended rodlike conformation,[31,34,36,37] which may be aligned under flowing conditions and produce a shear thinning effect.

The parameter $[\eta]^\bullet$ is usually nonzero for polyelectrolytes at sufficiently low ionic strength and tends to vanish when either the charge density over the macromolecule decreases or the medium ionic strength is high.[42] The influences of the py/Fe ratio on $[\eta]^\bullet$ values were the same as those for $[\eta]$, in agreement with Ghimici et al.[41] In this work, the authors varied the fraction of charged monomer units, analogous with the py/Fe ratio of the metallopolymers.

Crossed Effects of Solvatochromism and Viscosimetry. It was shown that the amount of pentacyanoferrate coordinated to P4VP tunes the polarity of the $[Fe(CN)_5]^{3-}$ microenvironment as well as the conformation of the macromolecule. It is now of interest to discuss how the solvation of pendant pentacyanoferrate influences the conformation and vice versa. A problem pointed out by Rice and Harris[43] in evaluating thermodynamic functions of a polyelectrolyte coil is the choice of a dielectric constant representative of the chemical environment of the electric charges separated from each other by a few angstroms inside the coil.

We thus expect that, by increasing the water molar fraction of the solvent of a metallopolymer with a fixed py/Fe ratio, the pentacyanoferrate solvation shell would become richer in water, increasing the dielectric constant of the microenvironment and resulting in stronger electric repulsion between $[Fe(CN)_5]^{3-}$ moieties. This electroviscous effect would lead to expansion of the coil. Besides, more water means better solvent quality for complexed repeating units, because they are hydrophilic overall.

On the other hand, more water means worse solvent quality for uncomplexed repeating units of 4-vinylpyridine, which are insoluble in water. This hydrodynamic effect would lead to shrinkage of the polymer coil because polymer−polymer interactions would be more favorable than polymer−solvent ones. Therefore, we hypothesize that these antagonistic effects may result in polymer coil shrinkage at either high or low solvent water contents. In order to confirm these hypotheses, the intrinsic viscosities of sample $[Fe(CN)_5(P4VP)_{25}]$ were measured with solvents with varied ethanol/water composition and compared with the solvatochromic shift at each solvent composition.

Figure 6a shows the experimental data adjusted by eq 10, and Table 5 presents the intrinsic viscosity values and the respective MLCT band energy.

When $[\eta]$ is plotted against X_{H_2O} in Figure 6b, one can note that $[\eta]$ decreases when X_{H_2O} approaches either 1 or 0, as expected, and it is approximately constant at X_{H_2O} from 0.244 to 0.642. At low X_{H_2O}, the hydrodynamic and electroviscous effect of complexed chain units are not favored because the ethanol-rich solvent does not suitably solvate $[Fe(CN)_5]^{3-}$ units and decrease the local dielectric constant, allowing ion pairing of $[Fe(CN)_5]^{3-}$ with Na^+. At high X_{H_2O}, the coil shrinkage may be explained because the solvent has turned into a bad solvent for uncomplexed repeating units of 4-vinylpyridine. Consequently, the best solvent quality is only found at intermediate X_{H_2O} values because both blocks of the macromolecule are suitably solvated.

Table 5. Intrinsic Viscosity Obtained by eq 10 and MLCT Energy (ν) of the Sample $[Fe(CN)_5(P4VP)_{25}]$ in Water/Ethanol Solvent at Varied Composition[a]

X_{H_2O}	$[\eta]$ (dL/g)	ν (10^3 cm^{-1})
0.928	0.41 ± 0.02	26.11 ± 0.07
0.829	3.9 ± 0.1	25.71 ± 0.07
0.642	4.0 ± 0.2	25.45 ± 0.07
0.447	4.4 ± 0.8	25.19 ± 0.06
0.224	3.7 ± 0.4	25.19 ± 0.06
0.114	3.0 ± 0.2	25.13 ± 0.06

[a]Correlation coefficients were all above 0.99.

Additionally, one can note in Figure 6 that $[\eta]$ is lower, or equivalently that the coil shrinks more in water-rich solvent (X_{H_2O} = 0.928) than in a water-poor solvent (X_{H_2O} = 0.114). This fact suggests that the hydrodynamic effect of uncomplexed 4-vinilpyridine repeating units is more pronounced than the contrary effects related to complexed units. A plausible explanation is the fact that there are 24 free repeating units for each one bearing a $[Fe(CN)_5]^{3-}$ complex; i.e., the molar fraction of free chain units (x_{4vpy} = 0.961) is much higher than that of the complexed units ($x_{Fe(CN)_5}$ = 0.039).

Figure 6c presents a plot of an intrinsic property of the macromolecule as a function of a property of the pendant $[Fe(CN)_5]^{3-}$ groups, so both the coil volume and the polarity of the complex chemical environment can be observed together. Here again, when the complex has more water in its solvation shell (MLCT band energy approaching 27.25 × 10^3 cm^{-1}), the coil shrinks, even with a higher dielectric constant to allow a stronger electrostatic repulsion. This result also corroborates the hypothesis that the solvation of the uncomplexed P4VP chain plays a more important role in coil expansion than electrostatic repulsion between $[Fe(CN)_5]^{3-}$ units. When X_{H_2O} gradually decreases, the polarity of the complex solvation shell also decreases and the coil expands up to a maximum where the opposing hydrodynamical effects counterbalance each other. At lower X_{H_2O}, the bad solvent quality for complexed units makes the coil shrink again.

■ CONCLUSIONS

The reaction between the water-soluble aminopentacyanoferrate(II) and the ethanol-soluble poly(4-vinylpyridine) yields a metallopolymer whose composition could be tuned from ∼3.5 to 400 polymer repeating units per complexed pentacyanoferrate moiety.

By virtue of compatibilization of molecular blocks of different solubility in the same macromolecule, the properties of each block were changed by the extension of the other. Solvatochromism of bound pentacyanoferrate showed that the longer the extent of pristine P4VP chain, the greater is the solvation by ethanol. Therefore, the chemical environment

polarity of $[Fe(CN)_5]^{3-}$ groups is tuned by the metallopolymer composition via an effect of the polymer coil.

Samples with high pentacyanoferrate content, such as $[Fe(CN)_5(P4VP)_5]$ and $[Fe(CN)_5(P4VP)_{10}]$, exhibit inversion of preferential solvation from ethanol to water when the medium is water-poor (X_{H_2O} < 0.42 and 0.25, respectively, Figure 4). This observation is rationalized assuming the formation of water pockets within the amphiphilic metallopolymer coils. This assumption motivated a modification of the preferential solvation model, allowing the prediction of the X_{H_2O} value where the inversion occurs.

The pentacyanoferrate content led, in turn, to an increase of intrinsic viscosity of the macromolecule due to steric hindrance and electrostatic repulsion of the bound $[Fe(CN)_5]^{3-}$ groups. Thus, the volume of the polymer coils is also tuned by the metallopolymer composition. Consequently, the accessibility to pentacyanoferrate groups is affected.

Finally, it was found that the solvent quality for uncomplexed chain segments plays a more important role in overall coil hydrodynamic volume than (i) the solvent quality for the $[Fe(CN)_5]^{3-}$-containing units and (ii) the electrostatic repulsion between nearby $[Fe(CN)_5]^{3-}$ groups.

AUTHOR INFORMATION

Corresponding Author

*E-mail: formiga@iqm.unicamp.br.

Notes

The authors declare no competing financial interest.

ACKNOWLEDGMENTS

S.A.V.J. and B.M. thank São Paulo State Research Foundation (FAPESP – grant numbers 2009/11903-6 and 2010/09127-5) for a fellowship and Prof. Dr. Bernhard Wolf and Pedro M. A. Rollo for helpful discussions. The National Counsel of Technological and Scientific Development (CNPq), the Coordenação de Aperfeiçoamento de Pessoal de Nível Superior (CAPES), and Petrobras are gratefully acknowledged. The authors thank Professor Carol H. Collins for her kind revision of the English in the manuscript.

REFERENCES

(1) Whittell, G.; Manners, I. *Adv. Mater.* **2007**, *19*, 3439–3468.

(2) Wang, X.; McHale, R. *Macromol. Rapid Commun.* **2010**, *31*, 331–350.

(3) (a) Liang, G.; Xu, J.; Wang, X. *J. Am. Chem. Soc.* **2009**, *131*, 5378–5379. (b) McHale, R.; Ghasdian, N.; Liu, Y.; Wang, H.; Miao, Y.; Wang, X. *Macromol. Rapid Commun.* **2010**, *31*, 856–860.

(4) (a) Culp, J.; Park, J.-H.; Stratakis, D.; Meisel, M.; Talham, D. *J. Am. Chem. Soc.* **2002**, *124*, 10083–10090. (b) Culp, J.; Park, J.-H.; Benitez, I.; Meisel, M.; Talham, D. *Polyhedron* **2003**, *22*, 2125–2131.

(5) Franco, C.; Paula, M. M. S.; Goulart, G.; de Lima, L.; Noda, L.; Gonçalves, N. *Mater. Lett.* **2006**, *60*, 2549–2553.

(6) (a) Lacroix, P.; Lin, W.; Wong, G. *Chem. Mater.* **1995**, *7*, 1293–1298. (b) Rawashdeh- Omary, M.; López-de-Luzuriaga, J.; Rashdan, M.; Elbjeirami, O.; Monge, M.; Rodríguez- Castillo, M.; Laguna, A. *J. Am. Chem. Soc.* **2009**, *131*, 3824–3825.

(7) Han, F. S.; Higuchi, M.; Kurth, D. G. *J. Am. Chem. Soc.* **2008**, *130*, 2073–2081.

(8) Shigehara, K.; Oyama, N.; Anson, F. *J. Am. Chem. Soc.* **1981**, *103*, 2552–2558.

(9) (a) Oyama, N.; Anson, F. *J. Am. Chem. Soc.* **1979**, *101*, 739–741. (b) Oyama, N.; Anson, F. *J. Am. Chem. Soc.* **1979**, *101*, 3450–3456.

(10) (a) Larsson, H.; Lindholm, B.; Sharp, M. *J. Electroanal. Chem.* **1992**, *336*, 263–279. (b) Sharp, M.; Larsson, H. *J. Electroanal. Chem.* **1995**, *386*, 189–195.

(11) Brauer, G. *Handbook of Preparative Inorganic Chemistry*, 2nd ed.; Academic Press: New York, 1963; Vol. *1*.

(12) Sharpe, A. G. *The Chemistry of Cyano Complexes of Transition Metals*; Academic Press: London, 1976.

(13) Toma, H.; Malin, J. *Inorg. Chem.* **1974**, *13*, 1772–1774.

(14) Toma, H.; Malin, J. *Inorg. Chem.* **1973**, *12*, 2080–2083.

(15) Nakamoto, K. *Infrared and Raman Spectra of Inorganic and Coordination Compounds, Part B*, 5th ed.; John Wiley and Sons: New York, 1997; Vol. *1*.

(16) Zhou, X.; Goh, S.; Lee, S.; Tan, K. *Polymer* **1997**, *38*, 5333–5338.

(17) Valkama, S.; Hartikainen, J.; Torkkeli, M.; Serimaa, R.; Ruokolainen, J.; Rissanen, K.; Ten Brinke, G.; Ikkala, O. *Macromol. Symp.* **2002**, *186*, 87–92.

(18) Sheng, K.; Yan, B. *J. Mater. Sci.: Mater. Electron.* **2010**, *21*, 65–71.

(19) (a) Macartney, D. L. *Rev. Inorg. Chem.* **1988**, *9*, 101–151. (b) Toma, H.; Malin, J. *Inorg. Chem.* **1973**, *12*, 1039–1045.

(20) Formation constants of $[Fe(CN)_5L]^{3-}$ complexes range from 10^5 to 10^6 L mol^{-1} in water. Apart from that, their solubilization in coordinating solvents usually results in dissociation that can be avoided only with an excess of free ligands. Reaction yields usually range from 70 to 90%.

(21) Toma, H.; Takasugi, M. *J. Solution Chem.* **1983**, *12*, 547–561.

(22) Baruah, B.; Roden, J.; Sedgwick, M.; Correa, N. b.; Crans, D.; Levinger, N. *J. Am. Chem. Soc.* **2006**, *128*, 12758–12765.

(23) Frankel, L.; Langford, C.; Stengle, T. *J. Phys. Chem.* **1970**, *74*, 1376–1381.

(24) Chanda, M. *Introduction to Polymer Science and Chemistry. A Problem Solving Approach*; CRC Press: Boca Raton, FL, 2006.

(25) Allen, G., Bevington, J. C., Eds. *Comprehensive Polymer Science: The Synthesis, Characterization, Reactions and Applications of Polymers*; Pergamon Press: Oxford, U.K., 1989; Vol. *1*.

(26) Wolf, B. *Macromol. Rapid Commun.* **2007**, *28*, 164–170.

(27) Morawetz, H. *Macromolecules in solution*, 2nd ed.; John Wiley Sons: New York, 1975.

(28) Huggins, M. *J. Am. Chem. Soc.* **1942**, *64*, 2716–2718.

(29) Booth, F. *Proc. R. Soc. London, Ser. A* **1950**, *203*, 533–551.

(30) Jiang, L.; Chen, S. *J. Non-Newtonian Fluid Mech.* **2001**, *96*, 445–458.

(31) Jiang, L.; Yang, D.; Chen, S. *Macromolecules* **2001**, *34*, 3730–3735.

(32) (a) Fuoss, R. *Science* **1948**, *108*, 545–550. (b) Fuoss, R. *J. Polym. Sci., Part A: Polym. Chem.* **1948**, *3*, 603–604. (c) Fuoss, R.; Strauss, U. *J. Polym. Sci.* **1948**, *3*, 602–603.

(33) Mansri, A.; Tennouga, L.; Desbrières, J. *Polym. Bull.* **2008**, *61*, 771–777.

(34) Vink, H. *Polymer* **1992**, *33*, 3711–3716.

(35) Cohen, J.; Priel, Z.; Rabin, Y. *J. Chem. Phys.* **1988**, *88*, 7111–7116.

(36) Yamanaka, J.; Araie, H.; Matsuoka, H.; Kitano, H.; Ise, N.; Yamaguchi, T.; Saeki, S.; Tsubokawa, M. *Macromolecules* **1991**, *24*, 6156–6159.

(37) Yamanaka, J.; Araie, H.; Matsuoka, H.; Kitano, H.; Ise, N.; Yamaguchi, T.; Saeki, S.; Tsubokawa, M. *Macromolecules* **1991**, *24*, 3206–3208.

(38) Witten, T.; Pincus, P. *Europhys. Lett.* **1987**, *3*, 315–320.

(39) Odijk, T. *Macromolecules* **1979**, *12*, 688–693.

(40) Samadi, F.; Wolf, B.; Guo, Y.; Zhang, A.; Schlüter, A. *Macromolecules* **2008**, *41*, 8173–8180.

(41) Ghimici, L.; Nichifor, M.; Eich, A.; Wolf, B. *Carbohydr. Polym.* **2012**, *87*, 405–410.

(42) Eich, A.; Wolf, B. *ChemPhysChem* **2011**, *12*, 2786–2790.

(43) Rice, S.; Harris, F. *J. Phys. Chem.* **1954**, *58*, 733–739.